Cycloidal Spin Order in the a-Axis Polarized Ferroelectric Phase of Orthorhombic Perovskite Manganite

Y. Yamasaki,[1] H. Sagayama,[2] N. Abe,[2] T. Arima,[2] K. Sasai,[3] M. Matsuura,[3] K. Hirota,[3] D. Okuyama,[4] Y. Noda,[2] and Y. Tokura[1,4,5]

[1]*Department of Applied Physics, University of Tokyo, Tokyo 113-8656, Japan*
[2]*Institute of Multidisciplinary Research for Advanced Materials, Tohoku University, Sendai 980-8577, Japan*
[3]*The Institute for Solid State Physics, University of Tokyo, Kashiwa 277-8581, Japan*
[4]*Multiferroics Project, ERATO, Japan Science and Technology Agency, University of Tokyo, Tokyo 113-8656, Japan*
[5]*Cross-Correlated Materials Research Group (CMRG), RIKEN, Wako, Saitama 351-0198, Japan*

(Received 7 May 2008; published 29 August 2008)

The ferroelectric state in an orthorhombic perovskite $R\mathrm{MnO_3}$ ($R = \mathrm{Gd_{0.7}Tb_{0.3}}$) was proved by neutron scattering studies to show the cycloidal spin state with the ab-spiral plane and the spin-helicity dependent polarization vector along the a axis, sharing the microscopic origin (inverse Dzyaloshinskii-Moriya interaction) with the more widely observed $P||c$ state (e.g., for $R =$ Tb and Dy) with the bc-spiral plane. The magnetic-field induced polarization flop from $P||c$ to $P||a$ as well known for $R\mathrm{MnO_3}$ is thus assigned to the orthogonal flop of the spin spiral plane from bc to ab.

DOI: 10.1103/PhysRevLett.101.097204 PACS numbers: 75.80.+q, 75.25.+z

There has been increasing interest in the multiferroic materials, in which ferroelectric order appears simultaneously with noncollinear magnetic ordering, due to their possibility of hosting the gigantic magneto-electric effect [1–3]. A number of systems have been shown to have concurrent magnetic and ferroelectric transitions, such as spiral magnets, $R\mathrm{MnO_3}$ ($R =$ Tb, Dy), $\mathrm{Ni_3V_2O_8}$, $\mathrm{MnWO_4}$, $\mathrm{LiCu_2O_2}$, and a transverse-conical magnet $\mathrm{CoCr_2O_4}$ [4–12]. Indeed, these systems commonly exhibit large magneto-electric effects, the orthogonal rotation of polarization, and/or the reversal of ferroelectric polarization by the application of magnetic field [4–9]. The ferroelectric feature is in accord with the inverse effect of Dzyaloshinsky-Moriya interaction (IDMI) which describes the relation between the polarization and the spin canting ($\boldsymbol{S}_i$ and $\boldsymbol{S}_j$) on neighboring two sites (i and j), $\boldsymbol{P}_{ij} \propto \boldsymbol{e}_{ij} \times \boldsymbol{C}_{ij}$ [13–16]. Here, $\boldsymbol{e}_{ij}$ denotes the vector connecting the two sites and $\boldsymbol{C}_{ij}$ the vector spin chirality, $\boldsymbol{C}_{ij} = \boldsymbol{S}_i \times \boldsymbol{S}_j$. On the basis of this mechanism, the direction of polarization should depend on the spin helicity, i.e., clockwise or counterclockwise. Recently, it was proven by a polarized neutron diffraction measurement in the spiral magnet $\mathrm{TbMnO_3}$ that the reversal of spin helicity (or vector chirality) is driven by an external electric field to form the single-domain state of the polarization [17].

One of the unresolved problems in multiferroic perovskite $R\mathrm{MnO_3}$ is the microscopic origin of the $P||a$ state with the commensurate magnetic modulation. In the ferroelectric phase of $\mathrm{TbMnO_3}$, for example, the application of the magnetic field along the b axis ($H||b$) induces a 90° rotation of polarization from $P||c$ to $P||a$ [4,18]. Although the coupling scheme between the magnetic order and the ferroelectricity in zero magnetic field has been established, the mechanism of the polarization flop and the magnetic ordering structure in the $P||a$ phase remain controversial. By synchrotron x-ray diffraction studies, the polarization flop was clarified to occur concomitantly with the incommensurate (IC, $q_m \sim 0.27$) to commensurate (C, $q_m = 0.25$) transition in the magnetic modulation wave vector $Q_l = (0\ q_m\ 1)$ [19–21]. Then, two possible magnetic structures are anticipated for this $P||a$ phase: the cycloidal order where spins rotate within the ab plane, or otherwise the collinear order where spins align along the a or b axis (↑↑↓↓ type) [19]. The $P||a$ can be explained by the IDMI model and by the exchange striction model, respectively. The latter model is applicable only when the wave number is C but anticipated to give a potentially very large $P(||a)$ value [22], whereas the former model can hold irrespective of whether the wave number is IC or C. In order to clarify the mechanism of the polarization flop for $\mathrm{TbMnO_3}$, the magnetic structure in this $P||a$ phase has to be determined at first. However, little is known about the specific magnetic structure partly because of the difficulty in analysis of magnetic structure in an external magnetic field.

To tackle this problem, we have taken an alternative approach and focused on the mixed-crystal system $\mathrm{Gd_{1-x}Tb_xMnO_3}$. The substituting of Tb ion with Gd ion of larger ionic radius leads to a successive decrease of the orthorhombic distortion, accompanied by an increase of the Mn-O-Mn bond angles governing the frustrated spin exchange interactions. Thus, the adjustment of the average ionic radius of the rare-earth site enables us to control the magnetic wave number. As a result, a ferroelectric $P||a$ phase appears in the $0.2 \leq x \leq 0.4$, while the crystal with $x \geq 0.4$ possesses a ferroelectric $P||c$ phase in the zero magnetic field [see the upper panel of Fig. 1(a)] [23]. When the magnetic field is applied along the b axis ($H||b$), the $P||a$ phase appears in the $0.2 \leq x \leq 1$ including $\mathrm{TbMnO_3}$

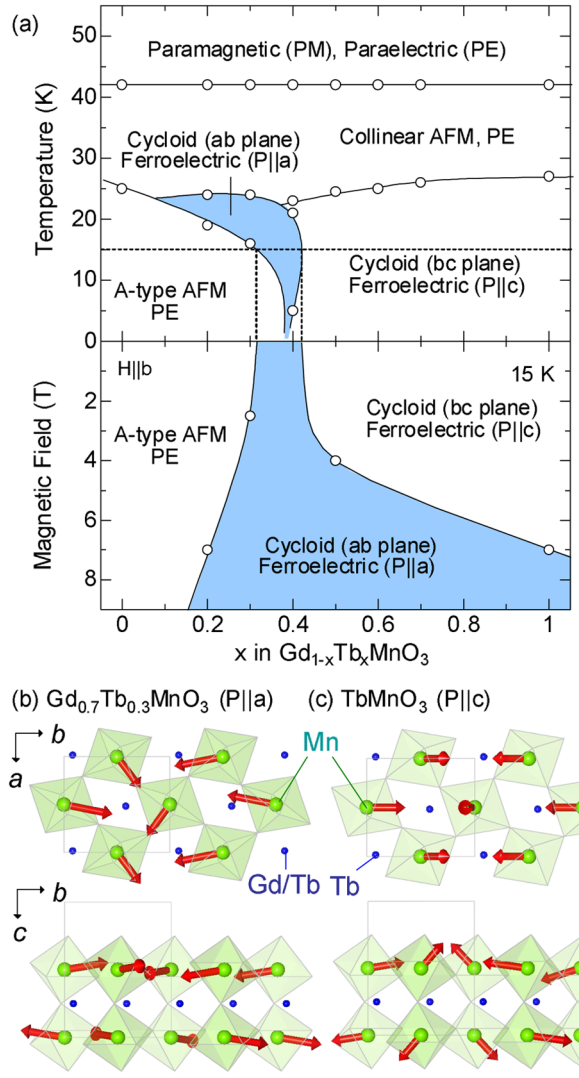

FIG. 1 (color online). (a) Magnetic phase diagram of perovskite $Gd_{1-x}Tb_xMnO_3$ in x-T plane (upper panel) and x-$H(||b)$ plane at 15 K (lower panel). The $x = 0.3$ compound, for example, undergoes the transitions, at first to the collinear antiferromagnetic (collinear AFM) and paraelectric (PE) phase at the Néel temperature T_N, then to the ferroelectric (FE) and cycloidal spin order phase at the Curie temperature T_C, and finally to the A-type antiferromagnetic (A-AFM) phase at T_A. (b) Cycloidal spin structure of the ferroelectric $P||a$ phase of $Gd_{0.7}Tb_{0.3}MnO_3$ ($x = 0.3$) revealed in this study; Mn spins rotate mostly within the ab plane with the commensurate magnetic wave number $q_m = 1/4$. (c) Cycloidal magnetic structure whose spins rotate within the bc plane with the incommensurate magnetic wave number $q_m \sim 0.27$ in the ferroelectric $P||c$ phase of $TbMnO_3$. Magnetic moments of rare-earth ions (Tb and Gd) are omitted in these figures.

and is identified to commonly emerge with a commensurate magnetic wave vector $Q_m = (01/41)$ [see the lower panel of Fig. 1(a)] [24,25]. In other words, the $H(||b)$-induced $P||a$ phase of $TbMnO_3$ is adiabatically connected to the zero-field $P||a$ phase of $Gd_{0.7}Tb_{0.3}MnO_3$, as clearly seen in the lower panel of Fig. 1(a); thus, both should share the same origin for the Mn-spin induced ferroelectricity with $P||a$. In this Letter, the magnetic structure and spin chirality for a single crystal $^{160}Gd_{0.7}Tb_{0.3}MnO_3$ [26] are investigated to uncover the coupling between the magnetic ordering and the ferroelectric polarization $P||a$ as well as to gain the clue to the mechanism of the magnetically induced polarization flop in $TbMnO_3$ and related compounds.

Figure 2 shows the temperature dependence of magnetization along the c axis ($M||c$), electric polarization along the a axis ($P||a$), and wave number of magnetic modulation (q_m) for $Gd_{0.7}Tb_{0.3}MnO_3$. This material undergoes the successive phase transitions, at first to the IC magnetic order phase at 40 K, then to the ferroelectric (FE) phase at 23 K, and finally to the A-type antiferromagnetic (A-AFM) phase (i.e., with the ferromagnetic ab planes coupled antiferromagnetically along the c axis) at 16 K. Both the magnetic and lattice modulations are observed in the intermediate temperature region of 16-40 K [see Fig. 2 (c)]. The ferroelectric ($P||a$) transition occurs concomitantly with the IC ($q_m \sim 0.24$) to C ($q_m = 0.25$) magnetic transition at 23 K [Figs. 2(b) and 2(c)]. Eventually, the q_m

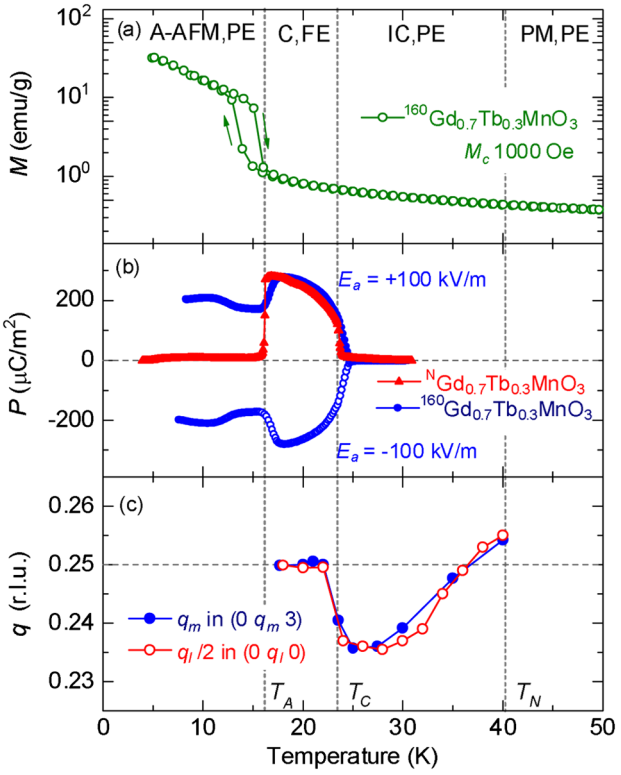

FIG. 2 (color online). Temperature dependence of (a) magnetization along the c axis ($M||c$), (b) electric polarization along the a axis ($P||a$) measured in a warming run after an electric field cooling procedure ($E = \pm 100$ kV/m), and (c) the magnetic wave number q_m in the neutron magnetic reflection (0 q_m 3) as well as derived from the lattice modulation wave number $q_l (= 2q_m)$ in the (0 q_l 0) synchrotron x-ray diffraction [24]. $^{160}Gd_{0.7}Tb_{0.3}MnO_3$ and $^{N}Gd_{0.7}Tb_{0.3}MnO_3$ denote the samples using ^{160}Gd and the naturally abundant Gd (^{N}Gd), respectively.

and the $P||a$ disappear upon the transition at 16 K to the A-AFM phase in which the tiny spontaneous magnetization along the c axis ($M||c$) exists due to the Dzyaloshinsky-Moriya interaction. There is a discrepancy in the $P||a$ between the ^{160}Gd-enriched and the normal samples; the $P||a$ disappears for the latter sample while not perfectly for the former in the A-AFM phase. Simultaneous observation of the $M||c$ and the $P||a$ may be accounted for the coexistence of the A-AFM and the FE phase because this material resides on the immediate vicinity of the boundary between these two phases. According to the result of the volume-sensitive neutron scattering (see below), the volume fraction of the $P||a$ phase in the nominal A-AFM phase is rather small (<10%), yet the un-negligible lattice effect arising from the isotopic substitution is also likely to be the origin of the phase coexistence at this Gd/Tb composition ratio.

A magnetic structural analysis was performed for the $P||a$ phase at 20 K in zero magnetic field. Single-crystal neutron diffraction measurements were carried out on a four-circle neutron diffractometer (FONDER) installed in the guidehall of JRR-3 at the JAERI, Tokai, Japan [27]. We collected 116 nuclear and 45 magnetic reflections at 20 K. The magnetic moments were calculated from the integrated-intensity data of the magnetic reflections by using a least-squared method. Figure 3(a) presents the comparison between the observed and calculated magnetic structural factors (F_{obs} and F_{cal}) of magnetic reflections at 20 K. The reliability factor R_I based on integrated intensities is 10.5%. The obtained magnetic structure is shown in Figs. 1(b) and 3(b). The a, b, and c components of the Mn spins modulate along the b axis with an amplitude of 2.0, 3.8, and $0.4\mu_B$, respectively. The phase of the modulation of the b components is shifted by $\pi/2$ from that of the a components, whereas it is the same as that of the c components. These results indicate that Mn spins represent the elliptical trajectory and rotate within the plane which is inclined slightly from the ab plane by $\sim \pm 6$ degrees. This transverse ellipsoidal alignment of spins breaks mirror reflection symmetry normal to the bc plane, in accordance with the occurrence of the $P||a$ state below T_C. In the similar fashion to $TbMnO_3$, the trajectory of the Mn spins is not a perfect circle but an ellipsoid with a ratio of the a- and b-component, m_a/m_b (ellipticity) ~0.53. The magnetic components of rare-earth ions modulate along the b axis and are parallel to the c axis with the amplitude of less than $1\mu_B$, and hence are not the origin of the electric polarization.

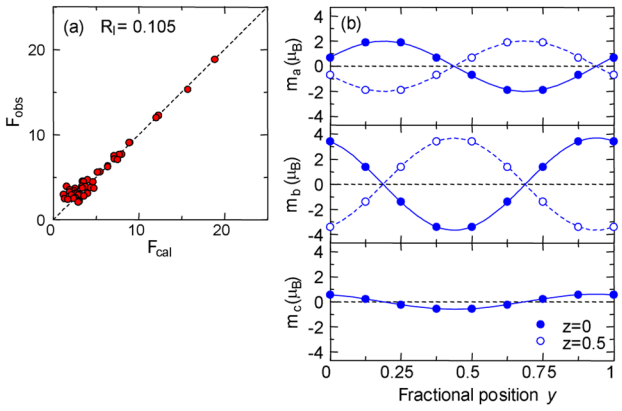

FIG. 3 (color online). (a) Comparison between observed (F_{obs}) and calculated (F_{cal}) structural factors of magnetic reflections of $^{160}Gd_{0.7}Tb_{0.3}MnO_3$ in the $P||a$ phase at 20 K. (b) Alignment of Mn-spin moments as a function of y (along the b axis) in the $a \times 4b \times c$ magnetic unit cell. Note that there are two basal Mn-O planes in a unit cell with $z = 0$ and 0.5 (along the c axis). The antiferromagnetic coupling in the a and b components and the ferromagnetic coupling in the c components between these two planes (i.e., mirror symmetry perpendicular to the c axis) are assumed.

To confirm the role of the cycloidal spin structure in the ferroelectric phase, we measured the electric field dependence of the spin helicity by a polarized neutron diffraction measurement. Measurements were performed with a triple-axis spectrometer PONTA at JRR-3 (for experimental details, see Ref. [17]). All the neutron diffraction measurements were performed without application of electric field once after cooling the sample from 50 K in a poling electric field (100 kV/m). Figures 4(a) and 4(b) show the K-scan profiles of magnetic satellites at $\boldsymbol{Q}_s = (0 + q_m 3)$ for the $P||a$ ferroelectric state at 20 K. In the case of $P_a > 0$ [Fig. 4(a)], the intensity is larger with the flipper off ($I_\uparrow$) than that with on ($I_\downarrow$). When the direction of the cooling electric field is reversed so as to cause the $P_a < 0$ state, the intensity with the flipper on ($I_\downarrow$) conversely becomes larger than that with off ($I_\uparrow$) [Fig. 4(b)]. The difference between $I_\uparrow$ and $I_\downarrow$ should be proportional to the scalar product of the scattering vector $\boldsymbol{Q}_s$ and the vector spin chirality $\boldsymbol{C} = \sum \boldsymbol{C}_{ij}$ [17]. The observed feature confirms the cycloidal spin structure with a single spin helicity, where the spiral plane is almost perpendicular to the scattering vector $\boldsymbol{Q}_s$. The spin helicity as determined by the relationship between $I_\uparrow$ and $I_\downarrow$ can thus be successfully controlled by the direction of the poling electric field applied in cooling. As depicted in Fig. 4(c), the magnetic satellite shows up below T_N, but there is no difference between $I_\downarrow$ and $I_\uparrow$ above T_C because of the sinusoidally modulated collinear spin structure in this IC and PE phase. The difference between $I_\downarrow$ and $I_\uparrow$ emerges upon the FE phase transition at T_C due to the cycloidal magnetic structure, evidencing that the $P||a$ occurs upon the collinear to cycloidal magnetic transition. The ellipticity is experimentally estimated as $m_a/m_b \sim 0.46$ using intensities measured at 20 K in the cooling process [28], in accord with the above-described result of the magnetic structure analysis ($m_a/m_b \sim 0.53$). In the low temperature phase below $T_A = 16$ K, the magnetic reflection (0 0 3) appears and the magnetic satellite reflections (0 q_m 3) almost disappear upon the transition to the A-AFM phase. The tiny residue of the (0 q_m 3) reflection below T_A is perhaps due to the residual FE phase coexistent with the A-AFM phase [29].

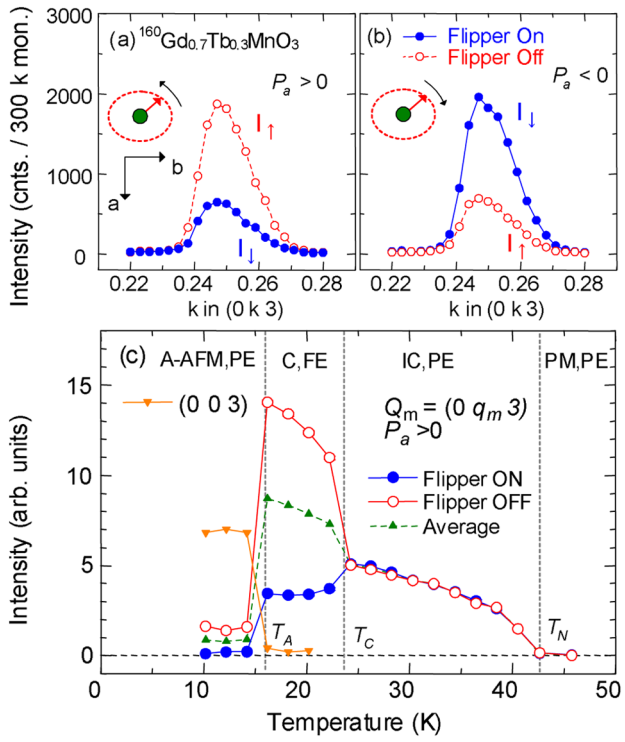

FIG. 4 (color online). (a) Profiles of polarized neutron magnetic satellite reflection (0 q_m 3) in the $P||a$ state of $^{160}Gd_{0.7}Tb_{0.3}Mn_3$ at 20 K; (a) $P_a > 0$ and (b) $P_a < 0$. Insets show the relation between the spin helicity and the direction of electric polarization. (c) The temperature dependence of $\boldsymbol{Q}$-integrated intensities of the magnetic reflections around $\boldsymbol{Q}$ = (0 q_m 3) and (0 0 3). The flipper off and on correspond to the incident neutron spin S_n parallel ($I_\uparrow$) and antiparallel ($I_\downarrow$), respectively, to the scattering vector $\boldsymbol{Q}_s$.

In summary, we have investigated the magnetic structure and the correlation between the spin-helicity and the electric polarization ($P||a$) for the ferroelectric $Gd_{0.7}Tb_{0.3}MnO_3$ by neutron diffraction measurements. The elliptic cycloid magnetic structure with the Mn spins rotating nearly within the ab plane was identified in the FE phase, providing that the $P||a$ is due to the inverse effect of Dzyaloshinsky-Moriya interaction, as well as in the case of the well-known $P||c$ state, and not due to the exchange striction effect in spite of its commensurate magnetic wave number $q_m = 0.25$. The same magnetic ordering is considered to be realized also for the magnetic-field-induced ferroelectric $P||a$ and commensurate phase of $TbMnO_3$ and related compounds, in which the change of the spins basal plane from the bc to ab plane is likely to cause the polarization flop from $P||c$ to $P||a$ by the application of magnetic field $H||b$ in $TbMnO_3$.

The neutron scattering experiments were carried out under the ISSP joint-research program. The authors are grateful to S. Seki, N. Soda, H. Katsura, and N. Nagaosa for enlightening discussions and to K. Ishii, N. Inami, and Y. Murakami for their helps in synchrotron x-ray measurements. This work was supported in part by Grants-In-Aid for Scientific Research (Grant No. 15104006, 17340104, 16076205, and 19052001) from the MEXT of Japan and JSPS.

[1] Y. Tokura, Science **312**, 1481 (2006).
[2] S.-W. Cheong and M. Mostovoy, Nature Mater. **6**, 13 (2007).
[3] T. Kimura, Annu. Rev. Mater. Res. **37**, 387 (2007).
[4] T. Kimura *et al.*, Nature (London) **426**, 55 (2003).
[5] T. Goto, T. Kimura, G. Lawes, A. P. Ramirez, and Y. Tokura, Phys. Rev. Lett. **92**, 257201 (2004).
[6] G. Lawes *et al.*, Phys. Rev. Lett. **95**, 087205 (2005).
[7] K. Taniguchi, N. Abe, T. Takenobu, Y. Iwasa, and T. Arima, Phys. Rev. Lett. **97**, 097203 (2006).
[8] S. Park, Y. J. Choi, C. L. Zhang, and S-W. Cheong, Phys. Rev. Lett. **98**, 057601 (2007).
[9] Y. Yamasaki *et al.*, Phys. Rev. Lett. **96**, 207204 (2006).
[10] G. Lawes *et al.*, Phys. Rev. Lett. **93**, 247201 (2004).
[11] M. Kenzelmann *et al.*, Phys. Rev. Lett. **95**, 087206 (2005).
[12] T. Arima *et al.*, Phys. Rev. Lett. **96**, 097202 (2006).
[13] H. Katsura, N. Nagaosa, and A. V. Balatsky, Phys. Rev. Lett. **95**, 057205 (2005).
[14] M. Mostovoy, Phys. Rev. Lett. **96**, 067601 (2006).
[15] I. A. Sergienko and E. Dagotto, Phys. Rev. B **73**, 094434 (2006).
[16] C. Jia, S. Onoda, N. Nagaosa, and J. H. Han, Phys. Rev. B **76**, 144424 (2007).
[17] Y. Yamasaki *et al.*, Phys. Rev. Lett. **98**, 147204 (2007).
[18] T. Kimura, G. Lawes, T. Goto, Y. Tokura, and A. P. Ramirez, Phys. Rev. B **71**, 224425 (2005).
[19] T. Arima *et al.*, Phys. Rev. B **72**, 100102(R) (2005).
[20] N. Aliouane *et al.*, Phys. Rev. B **73**, 020102(R) (2006).
[21] T. H. Arima, J. Phys. Soc. Jpn. **76**, 023602 (2007).
[22] I. A. Sergienko, C. Sen, and E. Dagotto, Phys. Rev. Lett. **97**, 227204 (2006).
[23] T. Goto, Y. Yamasaki, H. Watanabe, T. Kimura, and Y. Tokura, Phys. Rev. B **72**, 220403(R) (2005).
[24] T. Arima *et al.* (unpublished).
[25] Y. Yamasaki *et al.* (unpublished).
[26] A single crystal of $Gd_{0.7}Tb_{0.3}MnO_3$, with using ^{160}Gd to avoid the large neutron absorption cross section of naturally abundant Gd, was grown by a floating-zone method. The 98.6%-^{160}Gd-enriched Gd_2O_3 was purchased from ISOFLEX, USA.
[27] Y. Noda *et al.*, J. Phys. Soc. Jpn. **70**, A456 (2001).
[28] The ellipticity is estimated to the first approximation, $m_a/m_b = (\sqrt{I_\downarrow} - \sqrt{I_\uparrow})/(\sqrt{I_\downarrow} + \sqrt{I_\uparrow})$ (Ref. [17]), using the Q-integrated intensities $I_\uparrow \sim 12700$ and $I_\downarrow \sim 1760$ (in arbitrary units) which were observed during the cooling process.
[29] This residual phase appears to be present near the electrodes attached to the bc plane, judging from the fairy large contribution to the observed residual polarization [see Fig. 2(b)].